Bifurcations analysis of turbulent energy cascade

Nicola de Divitiis

"La Sapienza" University, Dipartimento di Ingegneria Meccanica e Aerospaziale, Via Eudossiana, 18, 00184 Rome, Italy

Abstract

This note discusses the mechanism of turbulent energy cascade through an opportune bifurcations analysis of the Navier–Stokes equations, and furnishes explanations on the more significant characteristics of the turbulence. A statistical property of the Navier–Stokes equations in fully developed turbulence is proposed, and a spatial representation of the bifurcations is presented, which is based on a proper definition of the fixed points of the velocity field. The analysis explains the mechanism of energy cascade through the aforementioned property as due to bifurcations, and gives reasonable argumentation of the fact that the bifurcations cascade can be expressed in terms of length scales, and that the local deformation is much more rapid than the fluid state variables. These properties, adopted as basic assumptions in previous works, are here justified through this bifurcations analysis. Next, the study provides a link between the order of magnitude of the critical Taylor–scale Reynolds number and the number of bifurcations at the onset of turbulence.

Keywords:
Energy cascade, Bifurcations, Fixed points, Lyapunov theory.

1. Introduction

The main aim of the work is to analyze the turbulent mechanism of energy cascade by means of specific properties of bifurcations of the Navier–Stokes equations. Moreover, through this analysis, we want to corroborate the basic hypotheses of previous works (de Divitiis (2010, 2013, 2012)) where the finite–scale Lyapunov theory is used to describe the homogeneous isotropic turbulence. There, the theory, which leads to the closure of von Kármán & Howarth (1938) and Corrsin (1951) equations, is based on the assumption that the bifurcations cascade law can be expressed in terms of the characteristic length scales of turbulence, and on the hypothesis that the relative kinematics between two contiguous particles is much faster than the fluid state variables. This latter, justified by the fact that, in turbulence, the kinematics of fluid deformation exhibits a chaotic behavior and huge mixing (Ottino (1989, 1990)), allows to express velocity and temperature fluctuations with Navier–Stokes and temperature equations, through the local fluid deformation (de Divitiis (2010, 2012)). The present work analyzes only the mechanism of kinetic energy cascade of an incompressible fluid in an infinite region, whereas does not consider the phenomenon of temperature cascade.

The work first introduces the bifurcations of the Navier–Stokes equations (NS–bifurcations), in line with the classical theory of differential equations (Ruelle & Takens (1971); Eckmann (1981)), and thereafter studies the phenomenon of energy cascade through a statistical property of the Navier–Stokes equations in regimes of fully developed chaos. This property, which represents an important element of this work, is based on basic characteristics of bifurcations. Next, to found the link between scales of turbulence and NS–bifurcations, the fixed points of the velocity field and the corresponding bifurcations (u–bifurcations) are properly defined. According to this definition, these u–bifurcations are shown to be non–material moving points which represent the trace of the NS–bifurcations in the fluid domain.

Through these elements, we furnish plausible argumentations that the NS–bifurcations are responsible for the main properties of turbulence, such as the chaotic fluid motion, the energy cascade, the continuous distribution of the length scales, and for the fact that the local fluid strain can be much more rapid than the fluid state variables. In particular, the aforementioned statistical property gives the link between NS–bifurcations and energy cascade mechanism, whereas the u–bifurcations justify the fact that the bifurcations cascade can be expressed in terms of length scales. Moreover, a description of the bifurcations cascade in terms of length scales is presented, which is based on properties of the route toward the chaos, and a relationship between the order of magnitude of the critical Reynolds number and number of bifurcations N at the transition is found. This estimation, based on adequate hypotheses about the length scales, gives $N = 3$ and the critical Taylor–scale Reynolds number $R_\lambda^* = 4 \div 14$, in agreement with the several theoretical and experimental sources of the literature. Next, R_λ^* is also determined beginning from the fully developed isotropic turbulence with the von Kármán–Howarth equation, by assuming the closure equation proposed by de Divitiis (2010) and a proper condition regarding the effect of the energy cascade. The two procedures give results in agreement with each other.

2. Bifurcations of the Navier–Stokes equations

This section studies the elements of the bifurcations of the Navier–Stokes equations for a homogeneous incompressible fluid in an infinite domain, which are necessary for the present analysis. The dimensionless equations are

$$\begin{aligned} &\nabla \cdot \mathbf{u} = 0, \\ &\frac{\partial \mathbf{u}}{\partial t} = -\mathbf{u} \cdot \nabla \mathbf{u} - \nabla p + Re^{-1} \nabla^2 \mathbf{u} \end{aligned} \tag{1}$$

where $Re = UL/\nu$ is the Reynolds number, $\mathbf{u}=\mathbf{u}(\mathbf{x}, t)$, and $p=p(\mathbf{x}, t)$ are dimensionless velocity and pressure, whereas U and L are the reference velocity and length. For sake of convenience, the momentum Navier–Stokes equations are formally written by eliminating the pressure field in Eqs. (1) through the continuity equation

$$\dot{\mathbf{u}} = \mathbf{N}(\mathbf{u}; Re) \equiv \mathbf{N}_0(\mathbf{u}) + Re^{-1} \mathbf{L}\mathbf{u} \tag{2}$$

where $\dot{\mathbf{u}}$ is the Eulerian time derivatives of the velocity field,

$$\mathbf{N} : \{\mathbf{u}\} \to \left\{ \frac{\partial \mathbf{u}}{\partial t} \right\} \tag{3}$$

is the nonlinear operator representing the R.H.S. of the momentum Navier–Stokes equations, and $\{\mathbf{u}\}$ and $\{\partial \mathbf{u}/\partial t\}$ are the sets of the fields $\mathbf{u}$ and $\partial \mathbf{u}/\partial t$, respectively. In Eq. (2), $\mathbf{N}_0(\mathbf{u})$ is the nonlinear operator which represents the inertia and pressure forces, whereas the linear operator $\mathbf{L}\mathbf{u}$ gives the viscosity term. In the case of homogeneous fluid in infinite domain, if $\mathbf{u}(\mathbf{x}, t)$ is a solution of Eq. (2), then $\mathbf{u}(\mathbf{x}+\mathbf{h}, t)$ satisfies Eq. (2), where $\mathbf{h}$ is an arbitrary displacement, i.e.

$$\dot{\mathbf{u}}(\mathbf{x}, t) = \mathbf{N}(\mathbf{u}(\mathbf{x}, t); Re) \quad \Rightarrow \quad \dot{\mathbf{u}}(\mathbf{x} + \mathbf{h}, t) = \mathbf{N}(\mathbf{u}(\mathbf{x} + \mathbf{h}, t); Re), \ \forall \mathbf{h} \tag{4}$$

In line with Ruelle & Takens (1971), we suppose that $\{\mathbf{u}\}$ can be replaced by a finite-dimensional manifold, thus Eq. (2) is here analyzed through the classical theory of the differential equations. Now, to define the bifurcations of the Navier–Stokes equations, observe that, if $Re = Re_0$ is properly small, the unique steady solution $\mathbf{u}(Re_0) = \mathbf{u}(\mathbf{x}; Re_0)$ is calculated by inversion of Eq. (2), whereas for higher values of Re, other steady solutions $\mathbf{u}(Re)$ can be obtained starting from $\mathbf{u}(Re_0)$, by applying the implicit function theorem to Eq. (2)

$$\mathbf{u}(Re) = \mathbf{u}(Re_0) - \int_{Re_0}^{Re} \nabla_{\mathbf{u}} \mathbf{N}^{-1} \frac{\partial \mathbf{N}}{\partial Re} \, dRe \tag{5}$$

where $\nabla_{\mathbf{u}} \mathbf{N} \equiv \partial \mathbf{N}(\mathbf{u}; Re)/\partial \mathbf{u}$ is the Jacobian of $\mathbf{N}$ with respect to $\mathbf{u}$. The velocity field $\mathbf{u}(Re)$ can be determined with Eq. (5) as long as $\nabla_{\mathbf{u}} \mathbf{N}$ is nonsingular, i.e. when the determinant $\det(\nabla_{\mathbf{u}} \mathbf{N}) \neq 0$.

The bifurcations of the Navier–Stokes equations occur when $\nabla_{\mathbf{u}} \mathbf{N}$ exhibits at least an eigenvalue with zero real part (NS–bifurcations). There, $\det(\nabla_{\mathbf{u}} \mathbf{N}) = 0$ thus, following Eq. (5), $\mathbf{u}(Re)$ can degenerate in two or more solutions. As the consequence of the structure of Eq. (2), we have the following route toward the chaos: For small Re, the viscosity forces are stronger than the inertia ones and $\mathbf{N}$ behaves like a linear operator with $\det(\nabla_{\mathbf{u}} \mathbf{N}) \neq 0$. When the Reynolds number increases, as long as $\nabla_{\mathbf{u}} \mathbf{N}$ is nonsingular, $\mathbf{u}(Re)$ exhibits smooth variations with respect to Re, whereas at a certain Re, this Jacobian becomes singular and $\partial \mathbf{u}/\partial Re$ appears to be discontinuous with respect to Re

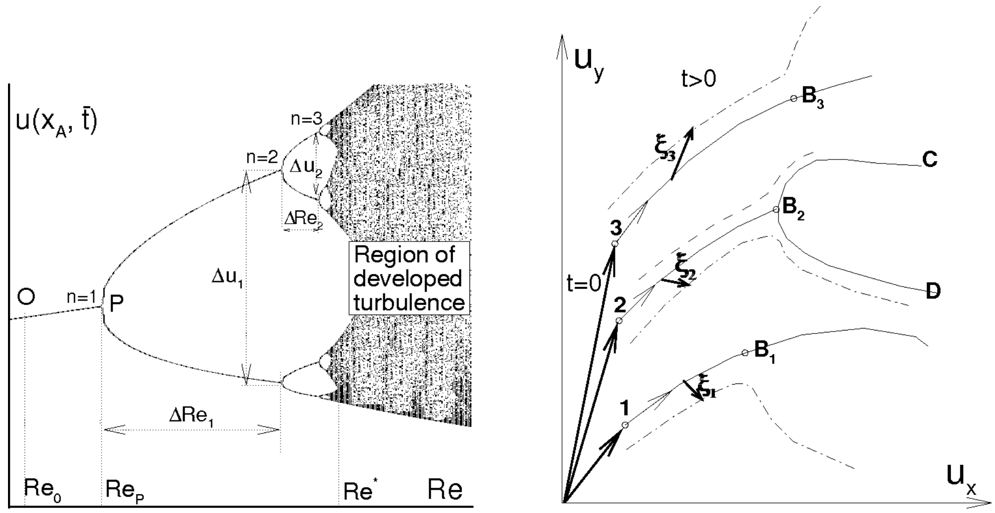

Figure 1: Left: qualitative scheme of NS–bifurcations. Right: qualitative scheme of phase trajectories in the hodograph plane.

(Guckenheimer (1990)). Of course, the route toward the turbulence can be of different kinds, such as, for example, those of Ruelle & Takens (1971), of Feigenbaum (1978), and of Pomeau & Manneville (1980). In general, the chaotic motion is observed when the number of encountered bifurcation is about greater than three. Figure 1 (Left) reports a qualitative scheme of the bifurcations tree, where a component of $\mathbf{u}(\mathbf{x}_A, \overline{t})$ is shown in function of Re, and $\mathbf{x}_A$ and $\overline{t}$ are assigned position and time. Starting from Re_0, the diagram is regular, until Re_P, where the first bifurcation determines two branches. Increasing again Re, other bifurcations occur. In the figure, Δu denotes the distance between two branches which born from the same bifurcation, ΔRe represents the distance between two successive bifurcations and n is the number of the encountered bifurcations starting from Re_0.

If the Reynolds number does not exceed the critical value Re^*, the velocity fields satisfying Eq. (5), are limited in number, thus also n is moderate. These branches, which give the intermediate stages of the route toward the chaos, form a tree whose overall dimension along u is of the order of Δu_1.

Conversely, when $Re > Re^*$, we have the region of developed turbulence. The diverse velocity fields satisfying Eq. (5), determine an extended complex geometry made by several points whose minimum distance is very small. This determines that the equation $\mathbf{N}(\mathbf{u}, Re)$ =0 is satisfied in a huge number of points of the velocity fields set which are very close with each other, whereas $\mathbf{N}(\mathbf{u}, Re) \neq 0$ elsewhere. Therefore, both the operators $\mathbf{N}$ and $\nabla_{\mathbf{u}}\mathbf{N}$ will exhibit abrupt variations on $\{\mathbf{u}\}$.

During the fluid motion, multiple solutions $\hat{\mathbf{u}}$ can be determined, at each instant, through inversion of Eq. (2)

$$\dot{\mathbf{u}} = \mathbf{N}(\mathbf{u}; Re)$$
$$\hat{\mathbf{u}}(Re) = \mathbf{N}^{-1}(\dot{\mathbf{u}}; Re) = \hat{\mathbf{u}}(Re_0) - \int_{Re_0}^{Re} \nabla_{\mathbf{u}}\mathbf{N}^{-1} \, \frac{\partial \mathbf{N}}{\partial Re} \, dRe \tag{6}$$

If $Re << Re^*$, $\mathbf{N}$ behaves like a linear operator, and Eq. (6) gives $\hat{\mathbf{u}} \equiv \mathbf{u}(\mathbf{x}, t)$ as unique solution, whereas if Re is properly high, $\mathbf{N}^{-1}$ is a multivalued operator and Eq. (6) determines several velocity fields $\hat{\mathbf{u}}$. That is, the current velocity field $\mathbf{u}(\mathbf{x}, t)$ corresponds to several other solutions $\hat{\mathbf{u}}(\mathbf{x}, t; Re)$ which give the same field $\dot{\mathbf{u}}(\mathbf{x}, t)$. For $Re > Re^*$ a huge number of these solutions are unstable, thus such solutions and the bifurcations determines a situation where $\mathbf{u}(\mathbf{x}, t)$ tends to sweep the entire velocity field set, accordingly the motion is expected to be chaotic with a high level of mixing.

From another point of view, when Re is given, a single NS–bifurcation corresponds to several phase trajectories bifurcations in the hodograph space and to a growth of the velocity gradient $\nabla_{\mathbf{x}}\mathbf{u}$. To show this, consider now the two velocity fields $\mathbf{u} = \mathbf{u}(\mathbf{x}, t)$ and $\mathbf{u}' = \mathbf{u}(\mathbf{x} + \mathbf{r}, t)$, where $\mathbf{r}$ is assigned. Their difference $\boldsymbol{\xi} = \mathbf{u}'$ - $\mathbf{u}$ varies with $\mathbf{x}$ and t. Taking into account the property (4) (homogeneous fluid in infinite space), $\mathbf{u}$ and $\mathbf{u}'$ are both solutions of Eq. (2), thus the evolution equation of $\boldsymbol{\xi}$ coincides with that of perturbation of the velocity field. If $r = |\mathbf{r}|$ is properly small, this equation reads as

$$\dot{\boldsymbol{\xi}} = \nabla_{\mathbf{u}} \mathbf{N}\, \boldsymbol{\xi} \tag{7}$$

where $\nabla_{\mathbf{u}} \mathbf{N}$ depends on $\mathbf{u}(\mathbf{x}, t)$ which in turn varies according to

$$\dot{\mathbf{u}} = \mathbf{N}(\mathbf{u}; Re) \tag{8}$$

For sake of convenience, we suppose that, at the onset of the motion, all the eigenvalues of $\nabla_{\mathbf{u}} \mathbf{N}$ exhibit negative real part, and that the NS–bifurcation happens for $t = t^* > 0$. There, at least an eigenvalue crosses the imaginary axis, and the phase trajectories, initially contiguous, thereafter diverge. Figure 1 (Right) shows three pairs of phase trajectories in the hodograph plane (u_x, u_y), each representing the velocity components in the pairs of points ($\mathbf{x}_1$, $\mathbf{x}_1 + \mathbf{r}$), ($\mathbf{x}_2$, $\mathbf{x}_2 + \mathbf{r}$) and ($\mathbf{x}_3$, $\mathbf{x}_3 + \mathbf{r}$), where the arrows denote increasing time. Continuous and dashed lines represent the velocities calculated in $\mathbf{x}_1$, $\mathbf{x}_2$, $\mathbf{x}_3$ and $\mathbf{x}_1 + \mathbf{r}$, $\mathbf{x}_2 + \mathbf{r}$, $\mathbf{x}_3 + \mathbf{r}$, respectively, whereas the points $\mathbf{B}_1$, $\mathbf{B}_2$, $\mathbf{B}_3$ give the velocities at $t = t^*$, thus these are the image of the NS–bifurcation in the hodograph plane. After the NS–bifurcation $\boldsymbol{\xi}_1(t)$, $\boldsymbol{\xi}_2(t)$ and $\boldsymbol{\xi}_3(t)$ diverge, and this means that a bifurcation causes a lost of informations with respect to the initial values $\boldsymbol{\xi}_1(0)$, $\boldsymbol{\xi}_2(0)$ and $\boldsymbol{\xi}_3(0)$ (Prigogine (1994)). In particular, for what concerns the single trajectory **2**–$\mathbf{B}_2$, after $\mathbf{B}_2$ it degenerates in the two branches $\mathbf{B}_2 - \mathbf{C}$ and $\mathbf{B}_2 - \mathbf{D}$ which represent two possible phase trajectories, thus $\partial \mathbf{u}/\partial t = 0$ in $\mathbf{B}_2$. After $\mathbf{B}_2$, Eq. (8) does not indicate which of the branches the fluid will choose, thus very small variations on the initial condition or little perturbations, are of paramount importance for the choice of the branch that the fluid will follow (Prigogine (1994)).

2.1. Local fluid deformation

This section gives reasonable argumentations that, in turbulence, the fluid deformation can be much more rapid than the fluid state variables. To show this, observe that $\boldsymbol{\xi}$ corresponds to variations of the velocity gradient $\nabla_{\mathbf{x}} \mathbf{u}$ which changes according to Eq. (7).

$$\frac{\partial \nabla_{\mathbf{x}} \mathbf{u}}{\partial t} = \nabla_{\mathbf{u}} \mathbf{N}\, \nabla_{\mathbf{x}} \mathbf{u} \tag{9}$$

where $\nabla_{\mathbf{x}} \mathbf{u}$ is formally expressed by

$$\nabla_{\mathbf{x}} \mathbf{u}(\mathbf{x}, t) = \exp\left(\int_0^t \nabla_{\mathbf{u}} \mathbf{N} dt \right) \nabla_{\mathbf{x}} \mathbf{u}(\mathbf{x}, 0) \tag{10}$$

This is the formal solution of Eq. (9), where the exponential denotes the series expansion of operators

$$\exp\left(\int_0^t \nabla_{\mathbf{u}} \mathbf{N} dt \right) = \mathbf{I} + \int_0^t \nabla_{\mathbf{u}} \mathbf{N}\, dt + ... \tag{11}$$

$\nabla_{\mathbf{x}} \mathbf{u}(\mathbf{x}, 0)$ is the initial condition, and $\mathbf{I}$ is the identity map. The bifurcations determine abrupt variations of $\nabla_{\mathbf{u}} \mathbf{N}$ which in turn produces an exponential growth of the velocity gradient according to Eq. (10). Thus, for $t > 0$, $\nabla_{\mathbf{x}} \mathbf{u}$ can exhibit non–smooth spatial variations, and $||\nabla_{\mathbf{x}} \mathbf{u}||$ is very high in a myriad of points of the fluid domain.

On the other hand, the local fluid deformation is related to the relative kinematics between two contiguous particles, and this link can be expressed through the Lyapunov theory. This kinematics is represented by the infinitesimal separation vector $d\mathbf{x}$ between the particles, which varies according to

$$d\dot{\mathbf{x}} = \nabla_{\mathbf{x}} \mathbf{u}\, d\mathbf{x} \tag{12}$$

The Lyapunov analysis of Eq. (12) gives the local deformation in terms of the maximal Lyapunov exponent $\Lambda > 0$

$$\frac{\partial \mathbf{x}}{\partial \mathbf{x}_0} \approx e^{\Lambda(t - t_0)} \tag{13}$$

where $\chi : \mathbf{x}_0 \rightarrow \mathbf{x}$ is the function which gives the current position $\mathbf{x}$ of a fluid particle located at the referential position $\mathbf{x}_0$ at $t = t_0$. As $||\nabla_{\mathbf{x}}\mathbf{u}|| >> 0$, the exponent $\Lambda \approx ||\nabla_{\mathbf{x}}\mathbf{u}||$ is expected to be high, thus according to Eq. (13) $\partial \mathbf{x}/\partial \mathbf{x}_0$ can be much faster than $\nabla_{\mathbf{x}}\mathbf{u}$ and $\mathbf{u}$, and can exhibit non–smooth spatial variations.

Remark. This property can have implications for what concerns the consequences of the basic formulation for deriving the Navier–Stokes equations. In fact, the Navier–Stokes equations are derived from an integral formulation of balance equations by means of the Green theorem, and this latter can be applied to regions which exhibit smooth boundaries during the motion (Truesdell (1977) and references therein). Now, if $\partial \mathbf{x}/\partial \mathbf{x}_0$ is much more rapid than $\mathbf{u}$ and exhibits abrupt spatial variations, the boundaries of fluid region become irregular in very short times, and this implies that the Navier–Stokes equations could require the consideration of very small scales and times for describing the fluid motion.

3. Fully developed chaos and energy cascade

To analyze the mechanism of energy cascade, this section presents a simple statistical property of the Navier–Stokes equations in the regime of fully developed chaos. This property, arising from basic elements of the bifurcations, is here applied to the Navier–Stokes equations in the form (2). To this purpose, consider now Fig. 2, where a scheme of two contiguous phase trajectories in the hodograph plane is shown in proximity of the trajectory bifurcation **B**. These phase trajectories correspond to velocity variations in two assigned points $\mathbf{x}_1$ and $\mathbf{x}_2 = \mathbf{x}_1 + \mathbf{r}$, where $r = |\mathbf{r}| > 0$

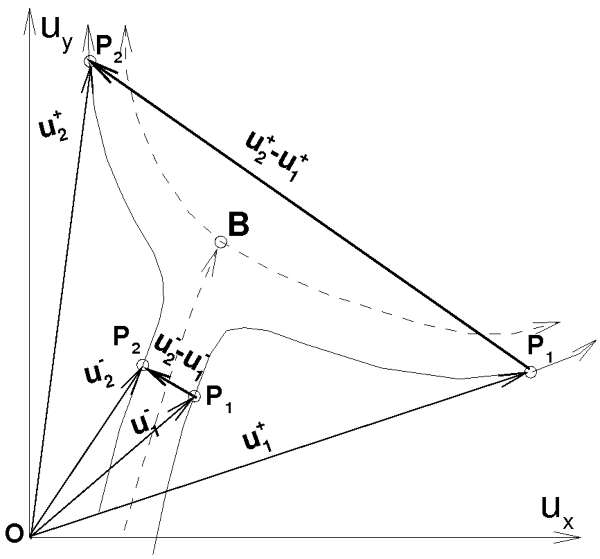

Figure 2: Scheme of the velocities variations near a bifurcation in the hodograph plane.

is arbitrarily small. The figure shows the velocity arrows P_1 and P_2 which describe the two phase trajectories, initially close with each other, that thereafter diverge because of the bifurcation. Let t^- and t^+ instants for which both P_1 and P_2 approach to **B** and move away from it, respectively. As the phase trajectories diverge

$$|\mathbf{u}_2^+ - \mathbf{u}_1^+| >> |\mathbf{u}_2^- - \mathbf{u}_1^-| \tag{14}$$

and, thanks to the bifurcation, $\det(\nabla_{\mathbf{u}}\mathbf{N}) = 0$, therefore we expect that

$$|\mathbf{u}_1^+| \approx |\mathbf{u}_1^-|, \quad |\mathbf{u}_2^+| \approx |\mathbf{u}_2^-| \tag{15}$$

The inequality (14) and Eq. (15) imply that

$$\mathbf{u}_1^+ \cdot (\mathbf{u}_2^+ - \mathbf{u}_1^+) << \mathbf{u}_1^- \cdot (\mathbf{u}_2^- - \mathbf{u}_1^-) \tag{16}$$

The condition (16) is frequentely satisfied in the chaotic regime, whereas the opposite inequality is possible but not probable. Hence, it is reasonable that

$$\frac{\partial}{\partial t} \langle \mathbf{u} \cdot (\mathbf{u}' - \mathbf{u}) \rangle \leq 0, \quad \forall r \text{ small} \tag{17}$$

Moreover, for relatively high values of r, due to the numerous phase trajectory bifurcations in between $\mathbf{x}_1$ and $\mathbf{x}_2$, the inequality (16) will be satisfied in average, therefore we assume that

$$\int_V \frac{\partial}{\partial t} \langle \mathbf{u} \cdot (\mathbf{u}' - \mathbf{u}) \rangle \; dV' \leq 0, \quad \forall \; V \tag{18}$$

where $\langle . \rangle$ denotes the average over the velocity ensemble and $dV' = dr_x dr_y dr_z$ is the elemental volume with $d\mathbf{r} = (dr_x, dr_y, dr_z)$. Taking into account Eq. (2), Eqs. (18) and (17) are both written in terms of $\mathbf{N}$

$$\begin{aligned} &\langle \mathbf{N} \cdot \Delta\mathbf{u} + \mathbf{u} \cdot \Delta\mathbf{N} \rangle \leq 0, \;\; \forall \; r \text{ small}, \\ &\int_V \langle \mathbf{N} \cdot \Delta\mathbf{u} + \mathbf{u} \cdot \Delta\mathbf{N} \rangle \; dV' \leq 0, \quad \forall \; V \end{aligned} \tag{19}$$

where now $\mathbf{u} = \mathbf{u}_1$, $\mathbf{u}' = \mathbf{u}_2$, $\mathbf{N} = \mathbf{N}_1$, $\Delta\mathbf{N} = \mathbf{N}' - \mathbf{N}_1$, $\Delta\mathbf{u} = \mathbf{u}' - \mathbf{u}$. Observe that Eq. (19) has been obtained from Eq. (2), for arbitrary $Re > Re^*$. Due to this arbitrarily and considering that the bifurcations are caused by the nonlinear terms of the Navier–Stokes equations, Eqs. (19) read as

$$\begin{aligned} &\langle \mathbf{N}_0 \cdot \Delta\mathbf{u} + \mathbf{u} \cdot \Delta\mathbf{N}_0 \rangle \leq 0, \quad \forall \; r \text{ small}, \\ &\int_V \langle \mathbf{N}_0 \cdot \Delta\mathbf{u} + \mathbf{u} \cdot \Delta\mathbf{N}_0 \rangle \; dV' \leq 0, \quad \forall \; V \end{aligned} \tag{20}$$

Equations (20) express the influence of bifurcations on the fluid motion.

At this stage of the analysis, we furnish adequate explanations that the bifurcations determine the transfer of kinetic energy from large to small scales. This is shown in case of homogeneous isotropic turbulence, by means of the evolution equation of the velocity correlation. This equation is obtained through the Navier–Stokes equations written in two points $\mathbf{x}$ and $\mathbf{x}' = \mathbf{x} + \mathbf{r}$, taking into account that, in such condition $\langle \mathbf{N}_0 \mathbf{u} \rangle \equiv 0$ (von Kármán & Howarth (1938))

$$\begin{aligned} &\frac{\partial}{\partial t} \langle \mathbf{u} \cdot \mathbf{u}' \rangle = Re^{-1} \left(2 \langle \mathbf{u} \cdot \mathbf{L}\mathbf{u} \rangle + \langle \mathbf{L}\mathbf{u} \cdot \Delta\mathbf{u} + \mathbf{L}\Delta\mathbf{u} \cdot \mathbf{u} \rangle \right) \\ &+ \langle \mathbf{N}_0 \cdot \Delta\mathbf{u} + \Delta\mathbf{N}_0 \cdot \mathbf{u} \rangle \end{aligned} \tag{21}$$

The first integral of Eq. (21) is the von Kármán & Howarth (1938) equation, the evolution equation of the longitudinal velocity correlation function. First and second terms at the R.H.S. of Eq. (21) give respectively, the rate of kinetic energy and the spatial variations of the velocity correlation due to the viscosity, whereas the third one, arising from the inertia forces, is responsible for the mechanism of energy cascade and identifies the term with the third–order statistical moment of velocity difference (von Kármán & Howarth (1938))

$$\langle \mathbf{N}_0 \cdot \Delta\mathbf{u} + \Delta\mathbf{N}_0 \cdot \mathbf{u} \rangle = \nabla \cdot \langle (\mathbf{u} \cdot \mathbf{u}')(\mathbf{u} - \mathbf{u}') \rangle \tag{22}$$

where

$$\lim_{r \to \infty} \langle \mathbf{N}_0 \cdot \Delta\mathbf{u} + \mathbf{u} \cdot \Delta\mathbf{N}_0 \rangle = 0, \quad \nabla \cdot \langle (\mathbf{u} \cdot \mathbf{u}')(\mathbf{u} - \mathbf{u}') \rangle = O(r^2) \text{ near } r = 0 \tag{23}$$

In homogeneous isotropic turbulence, $\nabla \cdot \langle (\mathbf{u} \cdot \mathbf{u}')(\mathbf{u} - \mathbf{u}') \rangle$ is an even function of r which vanishes for $r = 0$ (von Kármán & Howarth (1938)). According to the present analysis, Eq. (20) states that $\langle (\mathbf{u} \cdot \mathbf{u}')(u_r - u_r') \rangle$ and the skewness of the longitudinal velocity difference are both negative, and that the turbulent kinetic energy flows continuously from large to small scales, in agreement with the accepted idea of the mechanism of kinetic energy cascade (Batchelor (1953)). In fact, in line with von Kármán & Howarth (1938)

$$\frac{1}{r^2}\frac{\partial}{\partial r}\left(r^3 K(r)\right) \equiv \nabla \cdot \langle (\mathbf{u}\cdot\mathbf{u}')(\mathbf{u}-\mathbf{u}')\rangle \tag{24}$$

where $K(r)$ is an even function of r directly related to the longitudinal triple correlation function $k(r) = \langle u_r^2 u_r' \rangle / u^3$, according to

$$\frac{1}{r^4}\frac{\partial}{\partial r}(r^4 k(r)) = \frac{K(r)}{u^3} \tag{25}$$

where $u = \sqrt{\langle u_r^2 \rangle} \equiv \sqrt{\langle \mathbf{u}\cdot\mathbf{u}\rangle/3}$, and $u_r = \mathbf{u}\cdot\mathbf{r}/r$. Now, integrating Eq. (24) with respect to the volume V and taking into account Eq. (20) and that $K(0) = 0$, we have $K(r) < 0 \ \forall r > 0$, where due to isotropy, $dV' = dr_x dr_y dr_z = 4\pi r^2 dr$. Next, integrating Eq. (25) with $k(0) = 0$, we obtain $k(r) < 0 \ \forall r > 0$. Accordingly, the skewness of Δu_r and of $\partial u_r/\partial r$ are both negative

$$\begin{aligned} H_3(r) &= \frac{\langle (\Delta u_r)^3 \rangle}{\langle (\Delta u_r)^2 \rangle^{3/2}} \equiv \frac{6k(r)}{(2(1-f(r)))^{3/2}} < 0, \ \forall r > 0, \\ H_3(0) &= \lim_{r\to 0} H_3(r) = \frac{k^{III}(0)}{(-f^{II}(0))^{3/2}} < 0 \end{aligned} \tag{26}$$

where $f = \langle u_r u_r' \rangle / u^2$ is the longitudinal correlation function, and the superscript Roman numerals denote derivatives with respect to r. Furthermore, as $\nabla \cdot \langle (\mathbf{u}\cdot\mathbf{u}')(\mathbf{u}-\mathbf{u}')\rangle = O(r^2)$ near the origin, $H_3(0) < 0$ assumes a finite value.

In conclusion, the phenomenon of kinetic energy cascade is here explained with the proposed property (20) which deals with the bifurcations in the fully developed chaotic regime, and through the fact that $\mathbf{N}_0(\mathbf{u})$ really depends on the velocity gradient. Therefore, Eq. (20) provides the link between bifurcations and energy cascade mechanism and states that the bifurcations are the driving force of turbulence. Moreover, the condition that $\nabla \cdot \langle (\mathbf{u}\cdot\mathbf{u}')(\mathbf{u}-\mathbf{u}')\rangle$=0 in the origin, means that the bifurcations do not modify the average kinetic energy, but only influence the kinetic energy distribution at the different scales.

4. Fixed points and bifurcations of velocity fields

In order to analyze the link between NS–bifurcations and length scales of turbulence, the fixed points associated to the current velocity field $\mathbf{u}(\mathbf{x}, t) \in C^1(\{\mathbf{x}\} \times \{t\})$ are first introduced. These fixed points are defined as the points $\mathbf{X}$ satisfying

$$\hat{\mathbf{u}}(\mathbf{X}; Re) = 0, \tag{27}$$

where $\hat{\mathbf{u}}(\mathbf{X}; Re)$ is calculated with Eq. (6). To study these points, we recall that $\mathbf{u}(\mathbf{x}, t)$ corresponds to $\hat{\mathbf{u}}(\mathbf{x}; Re) = \mathbf{N}^{-1}(\dot{\mathbf{u}}; Re)$ which is not unique and depends on the Reynolds number. Thanks to this non–unicity and to the time variations of $\mathbf{u}(\mathbf{x}, t)$, these points continuously vary with the time. These points also depend on Re, and if $\mathbf{X}(Re_0)$ represents the fixed points calculated at $Re_0 << Re^*$, $\mathbf{X}(Re)$ can be formally obtained with the implicit function theorem

$$\mathbf{X}(Re) = \mathbf{X}(Re_0) + \int_{Re_0}^{Re} \nabla_{\mathbf{x}}\mathbf{u}^{-1} \nabla_{\mathbf{u}}\mathbf{N}^{-1} \frac{\partial \mathbf{N}}{\partial Re}\, dRe \tag{28}$$

where $Re > Re_0$. $\mathbf{X}(Re)$ can be determined with Eq. (28) if $\det(\nabla_{\mathbf{u}}\mathbf{N}\, \nabla_{\mathbf{x}}\mathbf{u}) \neq 0$. If we exclude the cases where $\det \nabla_{\mathbf{x}}\mathbf{u} = 0$, the u–bifurcations are defined as those fixed points where the operator $\nabla_{\mathbf{u}}\mathbf{N}$ admits at least one eigenvalue with zero real part. Hence, the u-bifurcations are the image of the NS–bifurcations in the fluid domain, and the previous considerations concerning the route toward the chaos can be applied to Eq. (28).

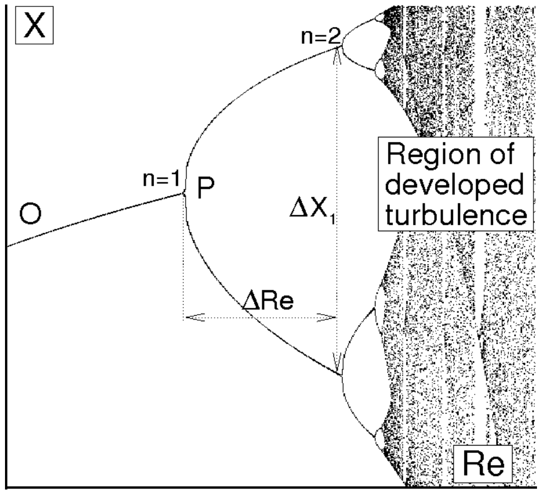

Figure 3: Qualitative scheme of bifurcations of a given velocity field.

Figure 3 shows a situation at a given instant $\bar{t}$ qualitatively similar to that of Fig. 1 (Right), where a component of $\mathbf{X}$ is reported in terms of Re following Eq. (28). In the figure, ΔX is the bifurcation scale, a length associated to each bifurcation which expresses the distance between branches which born from the same bifurcation. Such branches form a complex geometry which exhibits self–similarity as Re increases, whose overall dimension at the transition can be expressed as $X \equiv \Delta X_1 - \Delta X_N$ (Mandelbrot (2002); Mainzer (2005)). When $Re < Re^*$, the bifurcations are limited in number, and the sum of the distances between contiguous branches does not exceed X

$$\sum_{n \neq 1} \Delta X_n < \Delta X_1 - \Delta X_N \tag{29}$$

Vice versa, for $Re > Re^*$, the bifurcations frequentely happen and the several trajectories tend to describe the entire physical domain. As the result, the bifurcations tree will exhibit fractional dimension and self–similarity (Mandelbrot (2002); Mainzer (2005)), whereas the distance between the successive u–bifurcations is very small, and the sum of ΔX is greater than X (see for instance Mandelbrot (1967, 2002) and references therein), i.e.

$$\sum_{n \neq 1} \Delta X_n > \Delta X_1 - \Delta X_N \tag{30}$$

This situation corresponds to the current velocity field $\mathbf{u}(\mathbf{x}, \bar{t})$, where $\mathbf{u}(\mathbf{x}, t)$ follows the Navier–Stokes equations. As the result, we observe an unsteady motion depending on Re. Specifically, immediately before the transition ($Re \lesssim Re^*$), the motion is quasi–periodic characterized by a discrete distribution of independent basic scales ΔX and frequencies, each associated to a single bifurcation (Eckmann (1981) and refs. therein), whereas for $Re > Re^*$, the fluid motion is chaotic with a high level of mixing, the bifurcations behave like continuous transitions, where ΔX and frequencies play the role of real variables (Eckmann (1981) and refs. therein).

This spatial representation of NS-bifurcations and their continuous variations with respect to t, justify the continuous distribution of wavenumbers of the energy spectrum, and the assumption that the bifurcations cascade law can be expressed in terms of length scales (de Divitiis (2010)).

5. Bifurcations cascade in terms of length scales

The previous analysis justifies the fact that the bifurcations cascade can be expressed in terms of the scales ΔX. As these latter vary with time, their average values l_n are considered in function of n. Figure 4 qualitatively shows l_n immediately before the transition ($Re \lesssim Re^*$, filled symbols), where N is the number of encountered bifurcations at Re^*. These independent basic scales, discretely distributed, are represented by a given succession.

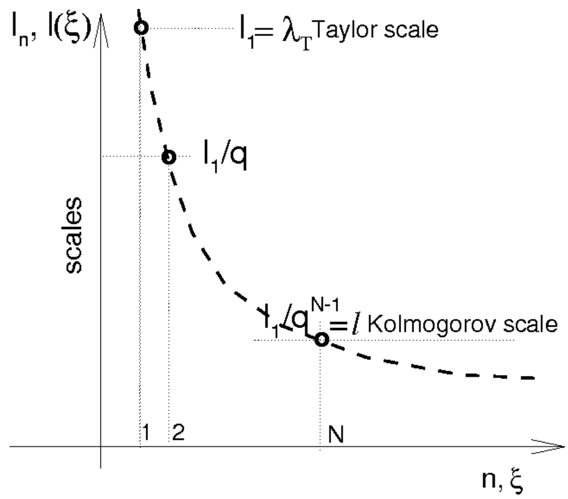

Figure 4: Filled symbols: Bifurcations cascade law for $Re \lesssim Re^*$. Dashed line: scales distribution for $Re \gtrsim Re^*$

Conversely, to represent the continuous scales l in developed turbulence, l is in terms of ξ, a real variable which replaces n and that expresses the continuous progress of the bifurcations in developed turbulence, where $\xi \in [1, N] \subset \mathbb{R}$, with $[\xi] = n$, and [.] denotes the integer part. Hence

$$l = l(\xi), \quad \xi \in [1, N] \subset \mathbb{R} \tag{31}$$

and $l(\xi)\ d\xi$ represents the elemental distance between neighbors transitions branches in developed turbulence.

For $Re << Re^*$, the flow is characterized by given frequency and spatial structure. Rising $Re < Re^*$, when the first bifurcation occurs, a new frequency, independent from the first one, appears together to the corresponding flow structure (Eckmann (1981); Gollub & Swinney (1975)). At the transition ($Re = Re^*$), the power spectra tend to become continuous, while their peaks preserve the frequencies immediately after the transition (Eckmann (1981); Gollub & Swinney (1975); Libchaber & Maurer (1979); Crutchfield et al (1980)). As these frequencies are associated to spatial structures of **u** through the Navier–Stokes equations, such preservation of peak frequencies corresponds to the keeping of the caracteristic scales of the velocity field through the transition. Therefore, the scales l_n obtained for $Re \lesssim Re^*$ maintain their values for $Re \gtrsim Re^*$ and ξ=n. Accordingly, the function $l(\xi)$ is chosen in such a way that

$$l(n) = l_n, \ n = 1, 2, ..., N \tag{32}$$

Next, because of the aforementioned self–similarity, l_n and $l(\xi)$ are supposed to be, respectively, a geometric progression and an exponential function, i.e.

$$\begin{aligned} l_n &= \frac{l_1}{q^{n-1}}, \quad n = 1, 2, ..., N, \ \text{for } Re \lesssim Re^* \\ l(\xi) &= \frac{l_1}{q^{\xi-1}}, \quad \xi \in [1, N] \subset \mathbb{R}, \ \text{for } Re \gtrsim Re^* \end{aligned} \tag{33}$$

where $q > 1$.

Now, the inequality (29) states that, for $Re \lesssim Re^*$, the sum of the distances ΔX does not exceed X, i.e.

$$\sum_{n=2}^{N} l_n < l_1 - l_N \equiv l_1 \left(1 - \frac{1}{q^{N-1}}\right) \tag{34}$$

On the contrary, for $Re \gtrsim Re^*$, the sum of such these distances is much greater than X (see ineq. (30)), and this can be expressed taking into account that $\xi \in \mathbb{R}$

$$\int_1^N l(\xi) d\xi > l_1 - l_N \equiv l_1 \left(1 - \frac{1}{q^{N-1}}\right) \tag{35}$$

Table 1: Critical Taylor–scale Reynolds number calculated for $N = 2, 3$, and 4, for different values of q.

q	Re^*_λ(N=2)	Re^*_λ(N=3)	Re^*_λ(N=4)
2.000	1.03	4.13	16.52
2.250	1.31	6.62	33.50
$\alpha \simeq 2.503$	1.62	10.13	63.49
e $\simeq$ 2.718	1.91	14.10	104.16

As $\{l_n, n = 1, 2, ...\}$ is a geometric succession, the inequality (34) is satisfied for $q > 2$ and N arbitrary, whereas the condition (35) is satisfied for $q < e$, that is

$$2 < q < e \tag{36}$$

6. Estimation of the critical Taylor–scale Reynolds number

In fully developed turbulence, the Taylor–scale Reynolds number is defined by

$$R_\lambda = \frac{u\lambda_T}{\nu} \tag{37}$$

where $\lambda_T = 1/\sqrt{-f^{II}(0)}$ is the Taylor scale. R_λ, λ_T and u are linked by means of the relation (Batchelor (1953))

$$\frac{\lambda_T}{\ell} = 15^{1/4}\sqrt{R_\lambda}, \tag{38}$$

where ℓ is the Kolmogorov microscale.

The critical Taylor–scale Reynolds number R^*_λ is first estimated starting from the route toward the chaos, using the bifurcations cascade seen at the previous section, and assuming an opportune property of the length scales. Thereafter, R^*_λ is also estimated beginning from the fully developed isotropic turbulence, adopting the closure equation presented in de Divitiis (2010) for the von Kármán–Howarth equation, and a plausible condition for f.

6.1. *Estimation of R^*_λ through the route toward the chaos*

To estimate R^*_λ through the route toward the turbulence, the relationship between R^*_λ and N is searched. Now, to obtain this link, it is worth to remark that, for $Re \gtrsim Re^*$, the minimum length $l(N)$, can not be less than the Kolmogorov scale ℓ, whereas $l(1) = \lambda_T$ (see Fig. 4), thus $\ell < l_n < \lambda_T$ for $Re \lesssim Re^*$, and

$$l_n = \frac{\lambda_T}{q^{n-1}}, \quad \ell = \frac{\lambda_T}{q^{N-1}} \tag{39}$$

Combining Eqs. (39) and (38), we have

$$R^*_\lambda = \frac{q^{2N-2}}{\sqrt{15}} \tag{40}$$

which expresses the searched relationship. With reference to table 1, all the values of R^*_λ calculated for $N = 2$, and $q \in [2, e]$, are of the order of the unity and this is not compatible with λ_T which represents the correlation scale, while the values $R^*_\lambda = 4 \div 14$ obtained for $N = 3$ and $q \in [2, e]$, are acceptable. In particular, if q is assumed to be equal to the second Feigenbaum constant ($\alpha = 2.502...$), $R^*_\lambda \simeq 10$. For $N = 4$, all the values of R^*_λ seem to be quite high in comparison with a plausible minimum values of R_λ, expecially for high values of q.

These orders of magnitude of R^*_λ calculated for $N = 3$, agree with the different theoretical routes to the turbulence (Ruelle & Takens (1971); Feigenbaum (1978); Pomeau & Manneville (1980); Eckmann (1981)), and with the diverse experimental data (Gollub & Swinney (1975); Giglio et al (1981); Libchaber & Maurer (1979)) which state that the transition occurs when $N \gtrsim 3$.

6.2. Estimation of R^*_λ through the fully developed turbulence

Next, to estimate R^*_λ starting from the regime of fully developed homogeneous isotropic turbulence, the solutions of the von Kármán–Howarth equation are considered in function of R_λ. To determine R^*_λ, we need an auxiliary condition which defines the lower limit for the existence of this regime of turbulence. To found this condition, observe that the homogeneous isotropic turbulence is an unsteady regime, where u and λ_T change with t according to (von Kármán & Howarth (1938); Batchelor (1953))

$$\frac{du^2}{dt} = -\frac{10u^2\nu}{\lambda_T^2} \tag{41}$$

$$\frac{5\nu}{\lambda_T^4} + \frac{1}{\lambda_T^3}\frac{d\lambda_T}{dt} = \frac{7}{6}uk^{III}(0) + \frac{7}{3}\nu f^{IV}(0) \tag{42}$$

where Eqs. (41) and (42) are the equations for the coefficients of the powers r^0 and r^2, respectively, of the von Kármán–Howarth equation. The term responsible for the energy cascade is the first one at the R.H.S. of Eq. (42), whereas the second one is due to the viscosity. According to Eq. (42), if the energy cascade is sufficiently stronger than the viscosity effects, then $d\lambda_T/dt < 0$. Hence, a reasonable condition to estimate R^*_λ can consist in to search the value of R_λ for which

$$\frac{d\lambda_T}{dt} = 0 \tag{43}$$

This value of R^*_λ depends on the adopted closure equation for K. If we use the results of the Lyapunov theory proposed by de Divitiis (2010), K is in terms of f and $\partial f/\partial r$

$$K = u^3\sqrt{\frac{1-f}{2}}\frac{\partial f}{\partial r} \tag{44}$$

thus Eq. (43) is satisfied for (Batchelor (1953))

$$R_\lambda \equiv R^*_\lambda = 2\left(\frac{7}{3}\varphi - 5\right) \text{ where } \varphi = \frac{f^{IV}(0)}{\left(f^{II}(0)\right)^2} \tag{45}$$

Following such estimation, R^*_λ is related to the behavior of f near the origin through $\varphi > 15/7$. For instance, when f is a gaussian function

$$f = \exp\left(f^{II}(0)\frac{r^2}{2}\right), \text{ then } \varphi = 3, \ \ R^*_\lambda = 4. \tag{46}$$

whereas if, according to the Kolmogorov law, f behaves like

$$f \approx 1 - cr^{2/3}, \quad c > 0, \text{ then } \varphi = 4.8, \ \ R^*_\lambda = 12.4. \tag{47}$$

where $f^I(\lambda_T/\sqrt{2})$ and $f^{II}(\lambda_T/\sqrt{2})$ are assumed to be equal to the corresponding derivatives of $1+1/2\, f_0^{II} r^2 + 1/4!\, f_0^{IV} r^4$ in $r = \lambda_T/\sqrt{2}$. These values are in qualitatively good agreement with those of the previous analysis based on the bifurcations.

7. Conclusion

We conclude this work by observing that the proposed statistical property of fully developed turbulence based on bifurcations, explains the energy cascade phenomenon in agreement with the literature, and motivates the fact that the local fluid deformation can be much faster than the velocity field. Furthermore, the spatial representation of the bifurcations justifies that the bifurcations cascade can be expressed in terms of length scales, and allows to argue that the scales are continuously distributed in developed turbulence. The proposed preservation of the bifurcation scales through the transition, leads to a link between critical Reynolds number and number of bifurcations at the transition, resulting N=3 and $R_\lambda^* \approx 4 \div 14$ in line with the literature. R_λ^* is also estimated as that value of the Taylor–scale Reynolds number which determines $d\lambda_T/dt = 0$ in the isotropic turbulence. The two procedures provide values of R_λ^* in agreement with each other.

8. Acknowledgments

This work was partially supported by the Italian Ministry for the Universities and Scientific and Technological Research (MIUR).

References

Batchelor, G.K., *The Theory of Homogeneous Turbulence*. Cambridge University Press, Cambridge, 1953.

Corrsin S., The Decay of Isotropic Temperature Fluctuations in an Isotropic Turbulence, *Journal of Aeronautical Science*, **18**, pp. 417–423, no. 12, 1951.

Crutchfield J., Farmer D., Packard N., Shaw R., Jones G., Donnelly R.J., Power spectral analysis of a dynamical system, *Physics Letters A*, **76**, 14, 1980.

de Divitiis, N., Lyapunov Analysis for Fully Developed Homogeneous Isotropic Turbulence, *Theoretical and Computational Fluid Dynamics*, DOI: 10.1007/s00162-010-0211-9.

de Divitiis, N., Refinement of a Previous Hypothesis of the Lyapunov Analysis of Isotropic Turbulence, *Journal of Engineering*, DOI: 10.1155/2013/653027.

de Divitiis, N., Finite Scale Lyapunov Analysis of Temperature Fluctuations in Homogeneous Isotropic Turbulence, *arXiv:1202.4113*.

Eckmann, J.P., Roads to turbulence in dissipative dynamical systems *Rev. Mod. Phys.* **53**, 643–654, 1981.

Feigenbaum, M. J., *J. Stat. Phys.* **19**, 1978.

Giglio M., Musazzi S., Perini U., Transition to chaotic behavior via a reproducible sequence of period doubling bifurcations, *Phys. Rev. Lett.* **47**, 243, 1981.

Gollub, J.P., Swinney, H.L., Onset of Turbulence in a Rotating Fluid., *Phys. Rev. Lett.* **35**, 927, 1975.

Guckenheimer, J., Holmes, P., *Nonlinear Oscillations, Dynamical Systems, and Bifurcations of Vector Fields*. Springer, 1990.

von Kármán, T., Howarth, L., On the Statistical Theory of Isotropic Turbulence., *Proc. Roy. Soc.* A, **164**, 14, 192, 1938.

Mainzer, K., *Symmetry And Complexity: The Spirit And Beauty Of Nonlinear Science*, World Scientific, 2005.

Mandelbrot B. B., How Long Is the Coast of Britain? Statistical Self-Similarity and Fractional Dimension, *Science*, **156**, 636–638, 1967, doi:10.1126/science.156.3775.636.

Mandelbrot, B. B., *Gaussian Self-Affinity and Fractals: Globality, The Earth, 1/f Noise, and R/S*, Springer, 2002.

Maurer, J., Libchaber A., Rayleigh–Bénard Experiment in Liquid Helium: Frequency Locking and the onset of turbulence, *Journal de Physique Letters* **40**, L419–L423, 1979.

Ottino, J. M. *The kinematics of mixing: stretching, chaos, and transport*, Cambridge Texts in Applied Mathematics, New York, 1989.

Ottino, J. M., Mixing, Chaotic Advection, and Turbulence., *Annu. Rev. Fluid Mech.* **22**, 207–253, 1990.

Pomeau, Y., Manneville, P., *Commun Math. Phys.* **74**, 189, 1980.

Prigogine, I., *Time, Chaos and the Laws of Chaos*. Ed. Progress, Moscow, 1994.

Ruelle, D., Takens, F., *Commun. Math Phys.* **20**, 167, 1971.

Truesdell, C. *A First Course in Rational Continuum Mechanics*, Academic, New York, 1977.